RGNZ/MGPB

Optimization of Stope Dimensions in a Geotechnically Complex Mine Using Automated Stability Analysis

Rudarsko-geološko-naftni zbornik
(The Mining-Geology-Petroleum Engineering Bulletin)
DOI: 10.17794/rgn.2026.2.3

Original scientific paper

Mohammad Army[1] ✉, Tri Karian[1]* ✉, Takashi Sasaoka[2] ✉, Akihiro Hamanaka[2] ✉, Firly Rachmaditya Baskoro[1] ✉, Budi Sulistianto[1] ✉, Hideki Shimada[2] ✉

[1] *Mining Engineering Department, Faculty of Mining and Petroleum Engineering, Institut Teknologi Bandung, Jalan Ganesha No.10, Bandung 40132, Indonesia.*

[2] *Earth Resources Engineering Department, Faculty of Engineering Department, Kyushu University, 744 Motooka, Nishi-ku, Fukuoka 819-0395, Japan.*

Abstract

Stope stability is a critical factor in underground mining, directly influencing safety, productivity, and overall mining efficiency. Traditional stope design methods often employ uniform stope lengths, disregarding geotechnical variability and thereby increasing the risk of instability or suboptimal dimensions. This study introduces an automated stability analysis approach that iteratively evaluates multiple stope dimension scenarios based on the Modified Stability Number (N') to identify the optimum stable configuration. By conducting detailed stability assessments for each stope wall, the method provides a more accurate representation of geotechnical conditions compared to the conventional methods with uniform stope length. The case study demonstrates that this approach effectively reduces the total number of stopes while maintaining geotechnical stability, in contrast to conventional methods where 14%–40% of stopes exhibit instability. Furthermore, the optimization method achieves a balanced outcome between dilution control and operational efficiency resulted in lower stope production cost. The optimized configurations generated by the proposed method deliver the lowest total production cost, with estimated savings of approximately USD 1.6–2.4 million compared to conventional designs. These findings confirm that the optimization framework not only enhances geotechnical stability but also provides a demonstrable economic advantage, underscoring the importance of integrating geotechnical variability into stope design.

Keywords:
stope stability, Modified Stability Number N', stope dimension optimization, automated analysis

1. Introduction

The stope stability during mining operations is a critical factor that directly influences both the safety and efficiency of underground mining activities (**Diederichs & Kaiser, 1996; Patanwar et al., 2025; Putra et al., 2024; Zhang et al., 2024**). Ensuring that the stope remains stable throughout the extraction process is essential to minimize the risks of ground failures, protect workers, and maintain uninterrupted production (**Adoko, 2025**).

The stability of a stope is significantly affected by its dimensions and the geotechnical characteristics of the surrounding rock mass (**Adoko, 2025; Cui et al., 2024; Li, Liu et al., 2024; Rinne et al., 2024; Sabao et al., 2022**). Larger stopes, while potentially lowering mining cost and increasing production efficiency, tend to be more susceptible to instability. In contrast, smaller stopes may enhance stability but can lead to higher costs (**Li et al., 2024; O'Hara & Suboleski, 1992**). Therefore, determining the optimum stope dimensions is crucial to achieving a balance between economic efficiency and geotechnical stability.

Traditionally, several mining operations adopt a simplified approach by applying a uniform stope dimension across different areas of the mine (**Chen et al., 2024; Guo & Miao, 2022; Heidarzadeh et al., 2019; Patanwar et al., 2025; Phaisopha et al., 2023; Zhao & Zhou, 2023**). These uniform dimensions are determined based on the general geomechanical properties of the rock mass (**Cui et al., 2024; Heidarzadeh et al., 2020; Kang et al., 2021; Nhleko & Musingwini, 2022**). This method was used due to its straightforward implementation, minimal computational requirements, and lack of necessity for detailed geotechnical data. Nevertheless, by generalizing stope dimensions across the entire mining area, this approach neglects the spatial variability of the rock mass, overlooking local differences in geomechanical characteristics. Such simplification can result in

* Corresponding author: Tri Karian
e-mail address: tri_karian@itb.ac.id
Received: 6 July 2025. Accepted: 1 October 2025.
Available online: 13 March 2026

Table 1. Advantage and disadvantage comparison

Method	Advantages	Disadvantages
Uniform stope dimension (Conventional method)	Simple implementation; low computational demand; widely adopted in practice	Ignores geotechnical variability of rock-mass; may cause local instability;
Stope dimension optimization using automated stability analysis (New method)	Considers spatial variability of the rock-mass; improves stability and cost efficiency	Detailed geotechnical data requirements; increased computational workload

suboptimal stope dimensions or even localized instability around individual stopes (**Zhou et al., 2023**).

In mining environments characterized by complex geotechnical conditions, the use of generalized stope dimensions can result in significant instability, particularly in areas of locally weak rock mass (**Cakrabuana et al., 2024; Zadhesh & Majdi, 2022; Zulfahmi et al., 2023**). This instability may lead to stope collapse and excessive overbreak, as documented in several case studies addressing dilution and overbreak in weak rock masses (**Clark, 1998**). For instance, at the Obuasi Mine in Ghana, local zones of poor rock mass and unfavourable structural conditions were identified as primary triggers for instability and excessive dilution (**Amedjoe & Agyeman, 2015**). Similarly, in the Dongguashan Copper Mine, China, unfavourable rock-mass structures, low mechanical properties, and excessive stope hydraulic radius were the leading causes of tall stope collapse (**Zhang et al., 2024**). Conversely, in a gold mine in Western Australia, the application of uniform stope dimensions, based on pessimistic assumptions, resulted in suboptimal design outcomes in areas with strong rock mass (**Stephenson & Sandy, 2013**). These cases underscore the necessity of addressing local ground weaknesses while optimizing stope dimensions in regions of stronger rock mass through the incorporation of spatial rock mass variability in both stability analysis and stope design.

This paper introduces an automated stability analysis method aimed at improving stope stability assessments and identifying optimum stope dimensions in a spatially distributed manner. The method involves iterating through various possible stope dimensions to determine the most stable configuration at each location within the mining area. To implement this method, an algorithm based on Modified Stability Number N' by **Potvin (1988)** will be used to streamline the analysis.

While this approach demands increased computational resources and more detailed geotechnical data, it offers significant potential benefits (**Dolatshahi & Molladavoodi, 2024; Sugianti & Tohari, 2023**). These include improved accuracy in stope stability assessments, reduced dilution rates, a decrease in the total number of required stopes, and, consequently, lower stope production costs. **Table 1** summarizes the principal advantages and disadvantages of the proposed automated stability analysis method in comparison with conventional uniform stope dimensioning practices.

The objective of this paper is to develop and validate an automated stability analysis method for optimizing stope dimensions in underground mining by incorporating spatial variability of rock mass properties into the design process. This approach aims to improve geotechnical stability, minimize the risk of stope failure, and achieve a balance between dilution control and operational efficiency. By iteratively evaluating multiple stope dimension scenarios using the Modified Stability Number (N'), the proposed method seeks to identify the most stable and cost-effective configurations, demonstrating significant economic benefits and enhanced safety compared to conventional designs that rely on uniform stope lengths.

2. Methods

2.1. Modified Stability Number

The stability analysis method utilized in this study is based on the modified stability number (N') introduced by **Potvin (1988)**, which builds based on the stability number developed by **Mathews et al. (1980)**. This original stability number is derived by adjusting the Q' value to account for factors such as induced stresses, the orientation of geological discontinuities, and the angle of the stope wall. The modified stability number, N', is calculated using **Equation 1**.

$$N' = Q' \times A \times B \times C \tag{1}$$

The rock stress factor (A) represents the strength of rock and the stress around the stope excavation. The joint orientation factor (B) assesses how the orientation of the primary joint set relates to the excavation surface, and the gravity adjustment factor (C) represents the influence of gravity on the stope wall stability. The values of these factors can be obtained using the chart shown in **Figure 1**.

An empirical approach is utilized to evaluate the stability or potential failure of stopes, wherein the hydraulic radius is correlated with the modified stability number (N'). This method is based on an extensive compilation of case histories originally developed by **Mathews et al. (1980)** and later refined by **Potvin (1988)**. The relationship is graphically represented in **Figure 2**, which categorizes stope conditions into three zones: stable, transition, and collapse. By plotting the N' value against the hydraulic radius, the chart provides a practical frame-

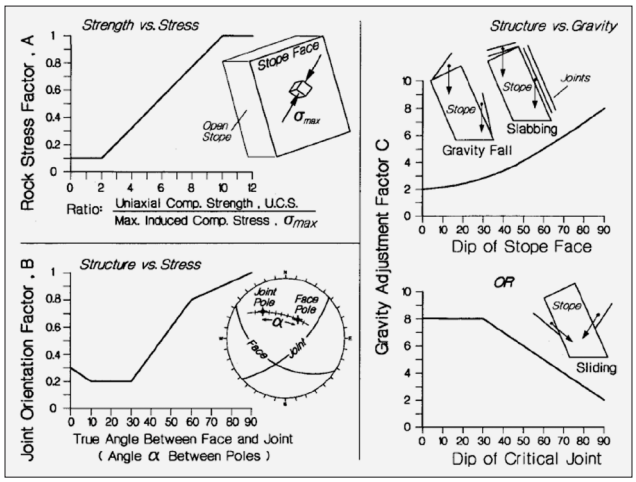

Figure 1. Factors A, B, and C by **Potvin (1988)**

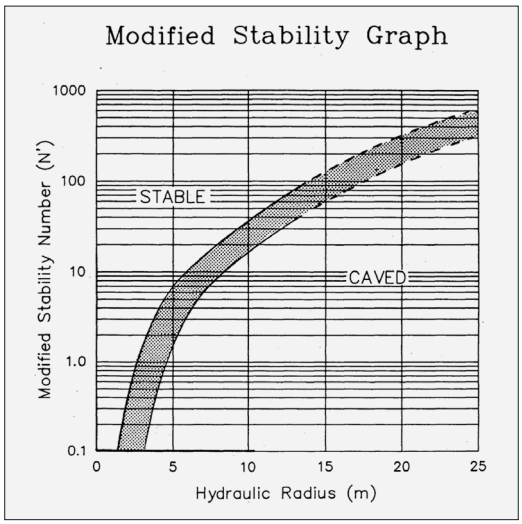

Figure 2. Modified stability graph by **Potvin (1988)**

work for assessing stope stability. This enables engineers to determine safe design dimensions for stope excavation.

2.2. Digitizing Graph Data

The linear approximation method will be used in this research to reconstruct several graphs from **Potvin (1988)** into mathematical functions. Most graphs were piecewise linear functions, making linear interpolation particularly suitable for accurately reproducing the trends without introducing artificial curvature. This method was chosen because the original datasets were only available as graphical plots, and linear interpolation offers simplicity, robustness, and low computational cost compared with higher-order polynomial or spline method, which can overfit local noise or produce unrealistic oscillations (**Press et al., 2007**). A sufficient number of points were sampled from each graph to ensure fidelity, and functions were constructed using **Equation 2** (**Salomon, 2006**). To determine the value of $f(x)$ using the interpolation method, find i such that $x_i \leq x \leq x_{i+1}$, then interpolate the value using **Equation 2**.

$$f(x) = f_i + \frac{x - x_i}{x_{i+1} - x_i}(f_{i+1} - f_i) \quad (2)$$

The accuracy of the digitization was evaluated using the Mean Absolute Error (MAE) for each function, summarized in **Table 2**. MAE values were below 0.5% in all cases, confirming that the reconstructed functions reliably represent the original graphs and are suitable for subsequent analysis. To further increase the accuracy of this method, additional sampling points can be incorporated, particularly in regions where the function changes rapidly (**Salomon, 2006**). Minor deviations may still occur due to image resolution or scaling effects.

Table 2. Number of Sampled Point and Mean Absolute Error (MAE)

Function	$f_N(HR)$	$f_A(SSR)$	$f_B(\alpha)$	$f_{Cj}(\alpha)$
Number of Sampled Point	8	10	6	200
Meam Absolute Error (MAE)	0.0%	0.0%	0.0%	0.4%

3. Stope Dimensions Optimization

As a mine can consist of dozens of stopes, with each stope containing dozens of possible dimensions, manually determining the stability of hundreds to thousands of possible stope dimensions is time-consuming (**Army & Karian, 2024**). To address this challenge, an algorithmic approach is implemented in this research**.** This process consists of several steps executed using Deswik, Python, and FLAC3D. The general workflow of the optimization process is illustrated in **Figure 3**.

The stope dimension optimization begins by discretizing a mineable stope boundary into individual slices, with the slice length corresponding to the minimum feasible blasting advanced. Each slice is first evaluated for stability, and unstable slices are excluded to prevent potential collapse during stopping (**Villaescusa, 2014**). Stable slices are then sequentially merged to progressively extend the stope geometry. After each merge, the stability of the resulting stope is assessed. If the stope remains stable, merging continues; if the addition of a slice induces instability, the merging process is terminated, and the last unstable slice is excluded. A new stope is subsequently initiated from the following slice. This merge–evaluate–terminate process is repeated until all the slices are assigned. Geometric discretization and modelling are performed in Deswik, iterative control is implemented in Python, and geomechanical parameters required for stability evaluation are derived from FLAC3D stress modelling. Details of the algorithm used in the optimization process are presented in **Section 3.1**,

while the stability assessment procedure is described in **Section 3.2**.

In this section, several terms and parameters were used; **Table 3** and **Figure 4** summarizes the notations and parameters that were used for the subsequent sections.

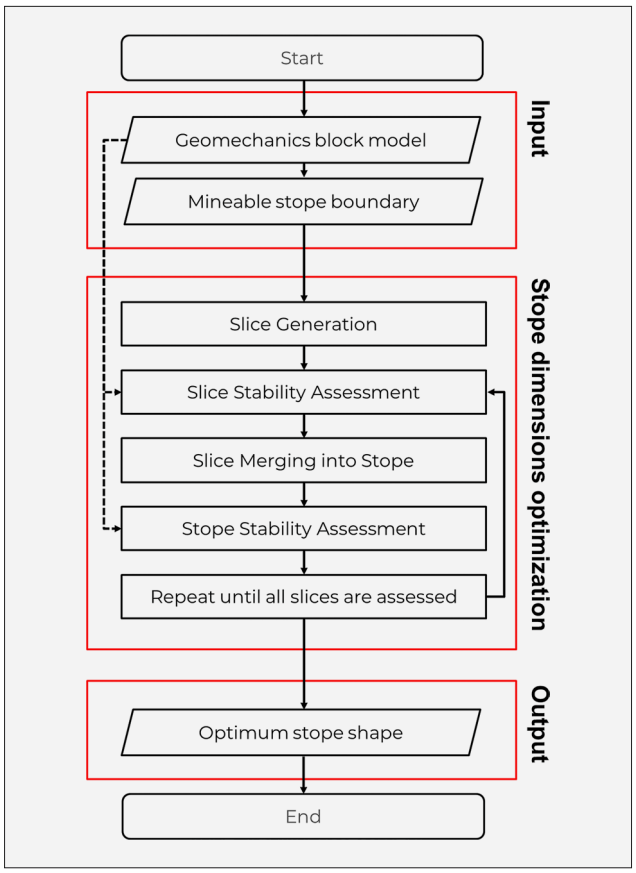

Figure 3. General workflow of the optimization process

3.1. Stope Shape Determination

Iterations will be conducted to determine the optimum stope shape. The objective of this optimization is to make the stope with the longest possible length, as described in **Equation 3**.

$$Objective\ function: Max(L_s) \tag{3}$$

Stope length is constrained by the stability of the stope, as a longer stope is more prone to instability. So, the optimum stope length must be verified as stable through a stability analysis, as described in **Equation 4**. The stope shape parameters, denoted as Shp_s comprise a numerical list representing the geometric and geotechnical attributes of the stope wall. The function f_{sta} serves as a binomial indicator of stope stability classification, where $f_{sta} = 1$ signifies the stope shape parameters resulted in stable stope, and $f_{sta} = 0$ mean stope shape parameters resulted in unstable stope. As previously outlined, the principal constraint in the optimization process is stope stability, necessitating that the resulting stope configuration satisfies $f_{sta}(shp_s) = 1$. Details about the stability analysis will be discussed in **Section 3.2**.

$$Constrain: f_{sta}(shp_s) = 1 \tag{4}$$

Based on the objective function and constraints, the pseudocode for the iteration is described in **Algorithm 1**. In the present algorithm, stability analysis is performed at each iteration to rigorously assess stope configurations. The computational complexity of this algorithm is O(N), where N represents the total number of stope slices, indicating a direct relationship between the process count and the number of slices evaluated. This systematic approach provides a robust framework for

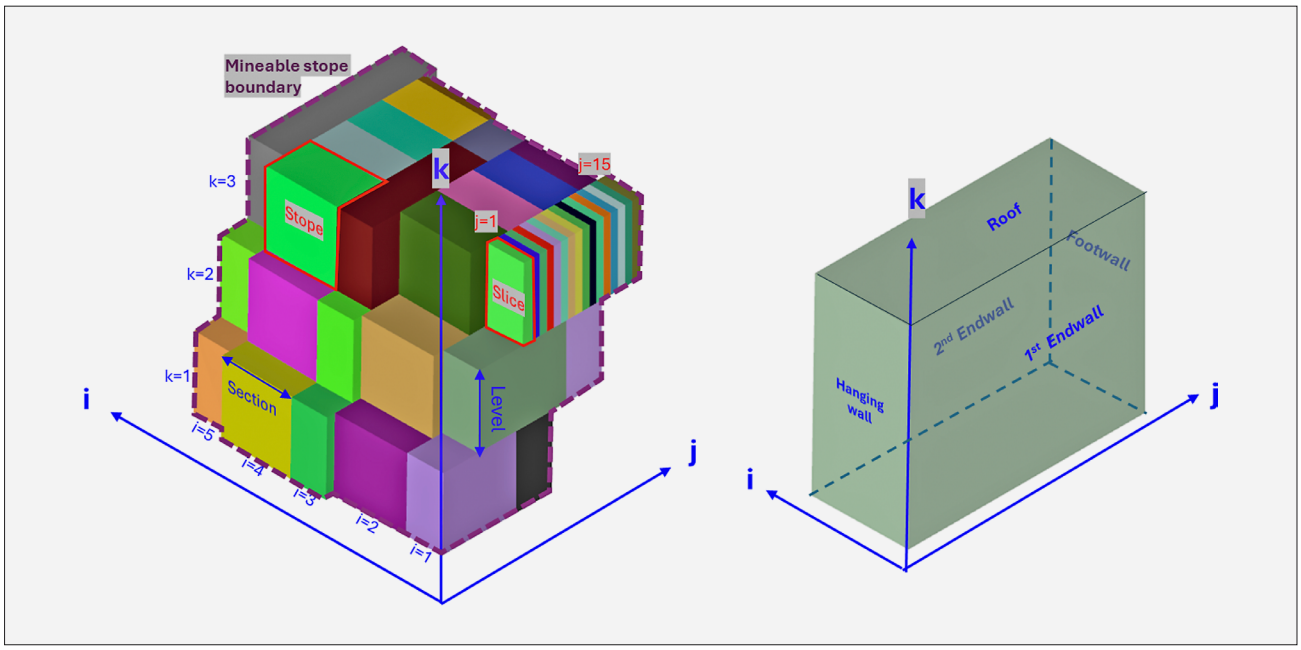

Figure 4. Notations and Parameters

Table 3. Notations and parameters

Symbol	Description
Notation	
x	Index of stope type. 1: Primary Stope 2: Secondary Stope
r	Index of block.
s	Index number of stope .
i	Index number of section.
j	Index number of Slice.
k	Index number of levels.
w	Index of stope wall. 0 : Hangingwall 1: Footwall 2 : Roof 3 : 1st End wall 4 : 2nd End wall
Parameters	
Sta_s	Stability of the stope s $[0,1]$. 1: $Stable\ stope\ shape$ 0: $Unstable\ stope\ shape$
sta_s^w	Stability of the wall w at stope s $[0,1]$. 1: $Stable\ stope\ wall$ 0: $Unstable\ stope\ wall$
shp_s	Shape of stope s.
$slice_{i,j,k}$	Shape of slice with index position of i,j,k
$st_{i,j,k}$	Stope number that belong to slice tag i,j,k. $st_{i,j,k} = -1$ mean slice won't be mined.
N_i	Number of section.
N_j	Number of slice.
N_k	Number of level.
Q_r	Q' value in block.
UCS_r	UCS in block.
Si_r	Induced stress in block.
Dd_r	Domain of discontinue orientation in block.
m_r^w	Proportion of the block influenced the stope wall *w*. $0 \le m_r^w \le 1$.
Wo_s^w	Norm vector of wall orientation of Stope *s* in wall *w*.
Wp_s^w	Perimeter of Stope *s* in wall *w*.
Wa_s^w	Area of Stope *s* in wall *w*.
Q_s^w	Q' value of Stope *s* in wall *w*.
UCS_s^w	UCS of Stope *s* in wall *w*.
Si_s^w	Induced stress of Stope *s* in wall *w*.
Dd_s^w	Domain of discontinue orientation of Stope *s* in wall *w*.
$\boldsymbol{Dd_{s,jo}^w}$	Normal vector of jo^{th} discontinue of Stope *s* in wall *w*.
A_s^w	Factor A value of Stope *s* in wall *w*.
B_s^w	Factor B value of Stope *s* in wall *w*.
C_s^w	Factor C value of Stope *s* in wall *w*.
N_s^w	N value of Stope *s* in wall *w*.

optimizing stope geometry while upholding structural stability throughout the evaluation process.

The proposed algorithm can be classified as a heuristic, constructive iterative algorithm designed to optimize stope geometry under explicit stability constraints. It operates by progressively merging stope slices and performing stability checks at each step, halting expansion once instability is detected. This rule-based process emphasizes computational efficiency and practical feasibility rather than exhaustive exploration of all possible configurations and therefore does not guarantee a globally optimal solution. Instead, it produces a locally optimal configuration that is inherently dependent on the sequence in which slices are evaluated. Due to the absence of backtracking, enumeration, or global search strategies, the algorithm is best described as greedy-like and heuristic, making it particularly suitable for practical applications in large scale mining scenarios where speed, simplicity, and reliable stability verification are prioritized over theoretical global optimality.

Algorithm 1: Stope Shape Iteration	
$s \leftarrow 1$	Initiation of stope number
$shp_s \leftarrow [\ \ ]$	Initiation of stope shape with blank shape
$for\ i = 1\ to\ N_i$	
$for\ k = 1\ to\ N_k$	
$for\ j = 1\ to\ N_j$	
$shp_s \leftarrow merge\,(\,shp_s, slice_{i,j,k})$	Merge the stope slice
$if\ f_{sta}(shp_s) = 1$	If stope shape stable
$st_{i,j,k} \leftarrow s$	Assign stope number s to slice tags i,j,k
$else$	
$shp_s \leftarrow slice_{i,j,k}$	
$s \leftarrow s + 1$	
$if\ f_{sta}(shp_s) = 1$	If slice stable
$st_{i,j,k} \leftarrow s$	Assign stope number s to slice tags i,j,k
$else$	
$st_{i,j,k} \leftarrow -1$	Assign -1 (unmined) to slice tags i,j,k
$shp_s \leftarrow [\ \ ]$	
$s \leftarrow s + 1$	
$shp_s \leftarrow [\ \ ]$	
$s \leftarrow s + 1$	

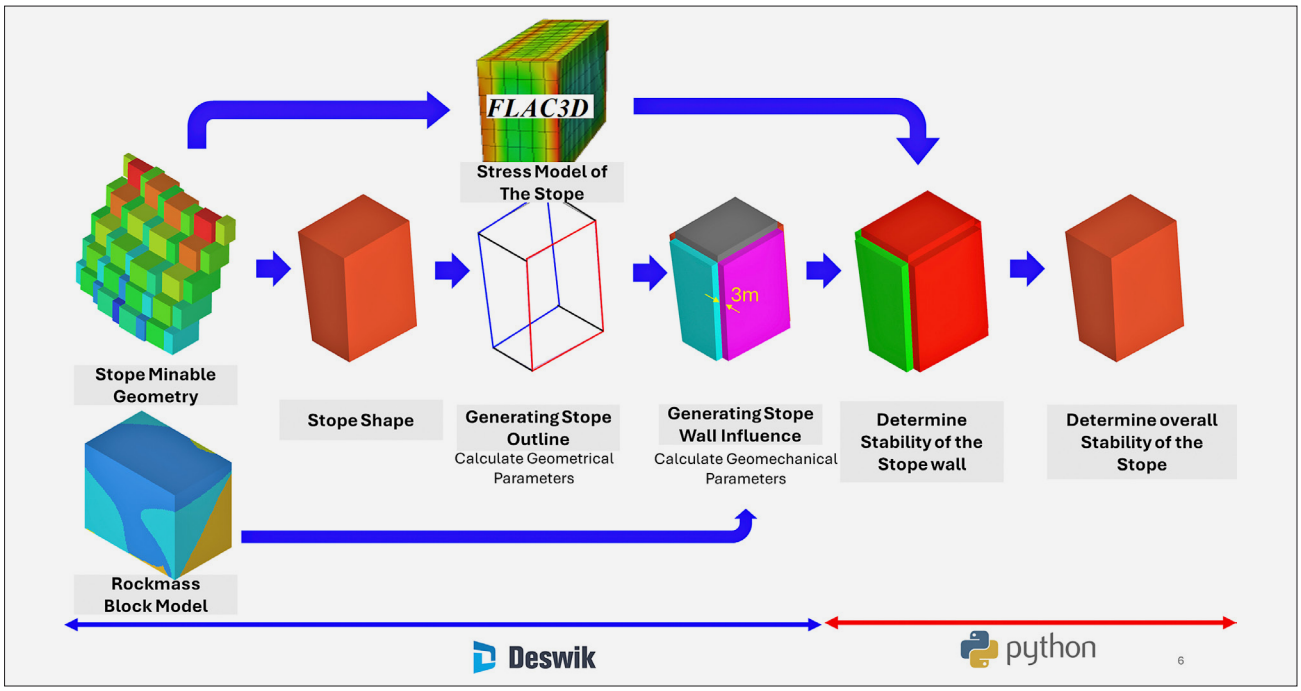

Figure 5. Stope shape stability workflow

3.2. Stability Evaluation

Based on the generated stope shape (Shp_s), several parameters will be generated to evaluate the stability of the stope. To determine these parameters, the outline of each stope wall will be generated to determine wall orientation, perimeter, and area. To define the representative rock mass properties for each stope wall, an n-meter boundary extension from the stope wall was applied, corresponding to the expected overbreak depth. Since the resulting stope is expected to be stable, the overbreak is anticipated to be less than 3 m (classified as large overbreak) based on **McFadyen et al. (2024)**. Therefore, the default value of n will be set to 3 m. This value remains consistent with the case study used in this research, considering the influence of stope geometry, stress conditions, and rock mass quality (**Cepuritis et al., 2007; Villaescusa, 2014**).

Subsequently, using the modelled stress of the stope, the wall orientation, and the rock mass properties of the stope wall, the N' value for each slice wall will be determined. This value is then used to evaluate the stability of each stope wall. The algorithm's general workflow is presented in the **Figure 5**, and the details of the stability evaluation will be discussed in this section.

As mentioned before, the stability of the stope is the function of several parameters, as described in **Equation 5**.

$$sta_s = f_{sta}(shp_s) = \\ = f_{sta}(Wo_s^w, Wp_s^w, Wa_s^w, Q_s^w, UCS_s^w, Si_s^w, Dd_s^w) \quad (5)$$

Wo_s^w, Wp_s^w, Wa_s^w are the geometrical parameters of the stope wall and the other parameter is the geotechnical parameters of the stope wall. The geotechnical parameters were generated from the block models and stress models using **Equations 6-9**.

$$Q_s^w = \frac{\sum Q_r \times tr \times m_r^w}{\sum tr \times m_r^w} \quad (6)$$

$$UCS_s^w = \frac{\sum UCS_r \times tr \times m_r^w}{\sum tr \times m_r^w} \quad (7)$$

$$Si_s^w = \frac{\sum Si_r \times tr \times m_r^w}{\sum tr \times m_r^w} \quad (8)$$

$$\boldsymbol{Dd_s^w} = \left\{ a \in \boldsymbol{Dd_r^w} \;\middle|\; \frac{\sum_{\boldsymbol{Dd_r^w}=a} tr \times m_r^w}{\sum tr \times m_r^w} > 0.1 \right\} \quad (9)$$

Given that $f_N(HR)$ is the function of stable boundary of minimum N' value for each HR from **Potvin (1988)** digitized graph. So, the stope wall stability can be determined using **Equations 10-12**.

$$N_s^w = Q_s^w \times A_s^w \times B_s^w \times C_s^w \quad (10)$$

$$HR_s^w = \frac{Wa_s^w}{Wp_s^w} \quad (11)$$

$$sta_s^w = \begin{cases} 1, & N_s^w \geq f_N(HR_s^w) \\ 0, & N_s^w < f_N(HR_s^w) \end{cases} \quad (12)$$

Equation 13 is then used to assess the stability of the stope.

$$sta_s = \begin{cases} sta_s^0 \times sta_s^1 \times sta_s^2 \times sta_s^3 \times sta_s^4, \ j = 1 \ and \ x = 1 \\ sta_s^1 \times sta_s^2 \times sta_s^3 \times sta_s^4, \ j > 1 \ and \ x = 1 \\ sta_s^0 \times sta_s^1 \times sta_s^2, \ j = 1 \ and \ x = 2 \\ sta_s^1 \times sta_s^2, \ j > 1 \ and \ x = 2 \end{cases} \quad (13)$$

3.3. Factor A determination

Given that $f_A\left(\frac{UCS}{\sigma_{max}}\right)$ is the function of Rock Stress factor **from Potvin (1988)** digitized graph, so the Factor A can be determined using **Equation 14**.

$$A_s^w = f_A\left(\frac{UCS_s^w}{Si_s^w}\right) \quad (14)$$

3.4. Factor B determination

Given that:

- $f_B(\alpha)$ is the function of the joint orientation factor from **Potvin (1988)** digitized graph
- $Dd_{s,jo}^w$ is the the norm vector of joint jo

So, Factor B can be determined using **Equations 15-16**.

$$\alpha_{s,jo}^w = cos^{-1}\left(\frac{\boldsymbol{Wo}_s^w \cdot \boldsymbol{Dd}_{s,jo}^w}{\| \boldsymbol{Wo}_s^w \| \| \boldsymbol{Dd}_{s,jo}^w \|}\right) \quad (15)$$

$$B_s^w = min\left(f_B\left(\alpha_{s,jo}^w\right) \forall \, jo \in \{0,1,2,3, \dots\}\right) \quad (16)$$

3.5. Factor C determination

Given that:

- $f_{Cs}(\alpha)$ is the function of the gravity adjustment factor of Stope face from **Potvin (1988).**
- $f_{Cj}(\alpha)$ is the function of the gravity adjustment factor of critical joint from **Potvin (1988)** digitized graph
- $\boldsymbol{Vo} = [\mathbf{0}, \mathbf{0}, \mathbf{1}]$ is the vector of vertical plane orientation.

So, Factor C can be determined using **Equations 17-22**.

$$f_{Cs}(\alpha) = 8 - 7 \times \cos(\alpha) \quad (17)$$

$$\alpha s_s^w = cos^{-1}\left(\frac{\boldsymbol{Wo}_s^w \cdot \boldsymbol{Vo}}{\| \boldsymbol{Wo}_s^w \| \| \boldsymbol{Vo} \|}\right) \quad (18)$$

$$\alpha j_{s,jo}^w = cos^{-1}\left(\frac{\boldsymbol{Vo} \cdot \boldsymbol{Dd}_{s,jo}^w}{\| \boldsymbol{Vo} \| \| \boldsymbol{Dd}_{s,jo}^w \|}\right) \quad (19)$$

$$Cs_s^w = f_{Cs}(\alpha s_s^w) \quad (20)$$

$$Cj_s^w = min\left(f_{Cj}\left(\alpha j_{s,jo}^w\right) \ \forall \, jo \in \{0,1,2,3, \dots\}, \ \alpha_{s,jo}^w < 30^0\right) \quad (21)$$

$$C_s^w = Q \, min(\{Cs_s^w, Cj_s^w\}) \quad (22)$$

4. Results

4.1. Geotechnical Data

This research utilizes a case study from a copper mine to demonstrate the proposed method. This case study was chosen because it highlights the importance of optimizing stope dimensions in areas where high productivity is required despite relatively poor ground conditions. Several geotechnical parameters were simplified and stored in the block model. The maximum dimensions of a regular block model are 10m × 10m, with parameter values estimated from drill hole data and laboratory test results. The geotechnical parameters considered in this study include:

- Geotechnical Domain
- Uniaxial Compressive Strength (UCS) (MPa)
- Q' Value
- Major Joint Orientation

The major joint orientation parameters are represented as integers that correspond to specific joint set codes. For example, joint set 1 represents a joint set with an orientation of 220°/45° NE. **Figure 6** illustrates the section view of the block model.

The copper deposit is hosted within a vein geotechnical domain, with 15 to 80 meters of apparent thickness. The vein generally trends about N 50° E and dips between 60° and 80°. The footwall belongs to a marble geotechnical domain, while the hanging wall consists of a diorite geotechnical domain.

The planned stopes are distributed across five levels, with 20 meters of vertical spacing between each level. The surface elevation is approximately 595 meters above sea level, placing the depths of the stope between 395 meters and 295 meters of elevation.

The geotechnical condition is relatively complex, with high variability in rock mass strength as summarized in **Table 4**. This variability results in significant differences in stope stability conditions, leading to a wide range of optimal stope dimensions.

4.2. Mining Method and Stope Sequence

The mining method used in this study is transverse longhole stoping with a primary and secondary stope sequence. This method is typically applied to ore bodies that are tabular and either vertical or steeply dipping. It is most effective when both the ore and the surrounding waste rock have fair to good rock quality (**SME, 2011**).

In this method, the stope design consists of two types of stopes: primary stopes and secondary stopes. The primary stopes are mined first and then backfilled with cemented backfill, serving as pillars when the secondary stopes are later mined, as presented in the **Figure 7**. Different sizes of primary and secondary stopes are applied in this study, and their dimensions are presented in **Table 5**.

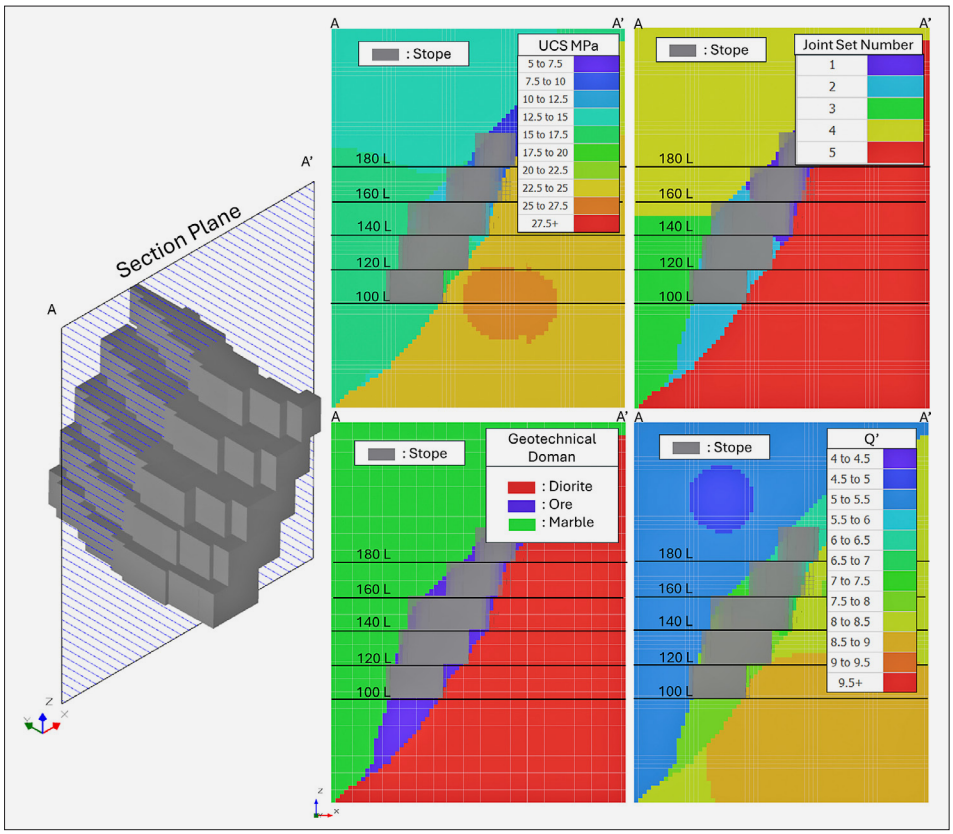

Figure 6. Block model of geotechnical data

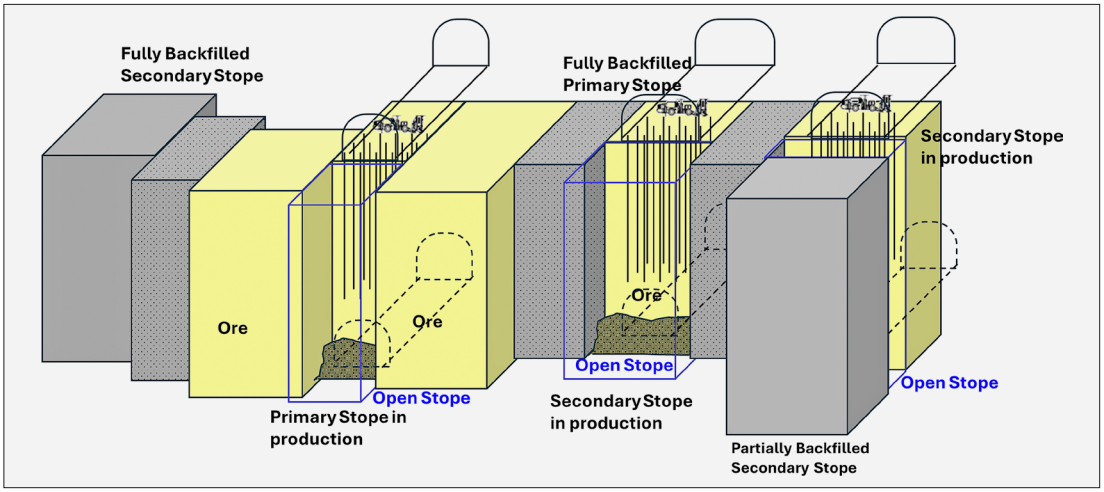

Figure 7: Mining method

Table 4. Summary of the rock mass properties

Parameters	Symbol	Minimum	Maksimum
UCS (MPa)	UCS_r	5.1	28.5
Q'	Q_r	4.4	9.2
Rock Domain	Rd_r	{Diorite, Ore, Marble}	
Joint Set Domain	Dd_r	{1,2,3,4,5}	

Table 5. Stope dimension

Stope	Width (m)	Height (m)
Primary	10	20
Secondary	20	20

This method was selected because the ore body thickness exceeds 60 meters, necessitating an efficient, large-scale mining approach. A partial backfill stope approach is implemented in certain areas where the ore body is too thick to be mined in a single stope sequence. In these cases, the stope is divided into multiple sections, and each section must be backfilled before mining the next section.

The stope sequence follows an overhand stoping sequence, meaning that a stope can only be mined once the stope below it has already been mined and backfilled. Additionally, a primary-secondary stoping dependency is enforced, where a secondary stope can only be mined

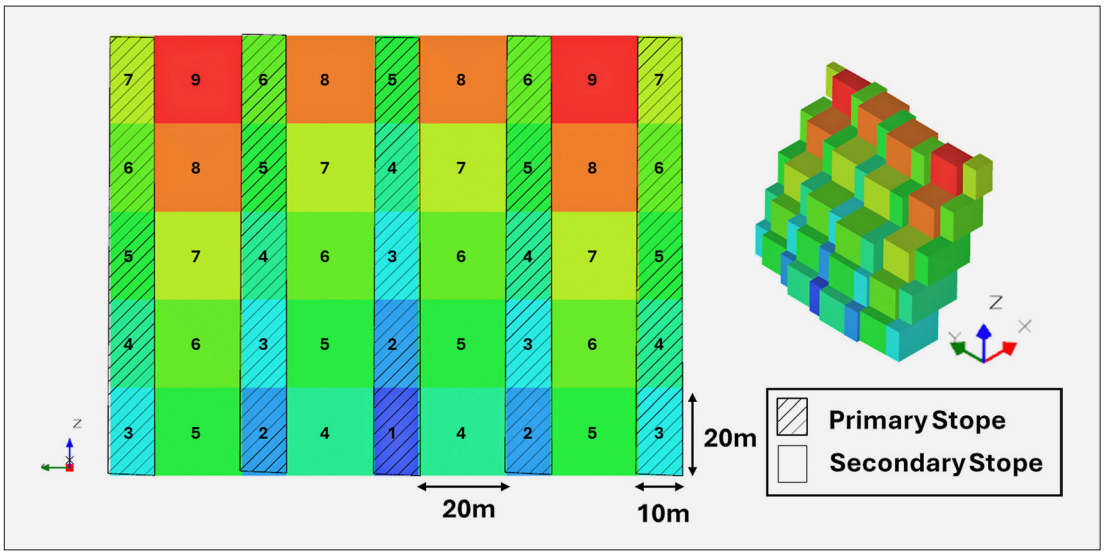

Figure 8. Stopping sequence

Table 6. Material properties of the model

Property	Granodiorite (Footwall)	Marble (Hanging wall)	Ore body	Cemented tailings (Backfill)
Unit weight (kN//m³)	28	28	30	22.1
Uniaxial Compressive Strength (MPa)	23	17	15	3.5
Tensile Strength (MPa)	1.0	0.8	1.7	0.5
Cohesion (MPa)	6.0	2.1	4.3	0.65
Internal Friction angle (°)	43	40	41	35
Young's Modulus (MPa)	7800	18600	39000	1000
Poisson's Ratio	0.16	0.26	0.31	0.30

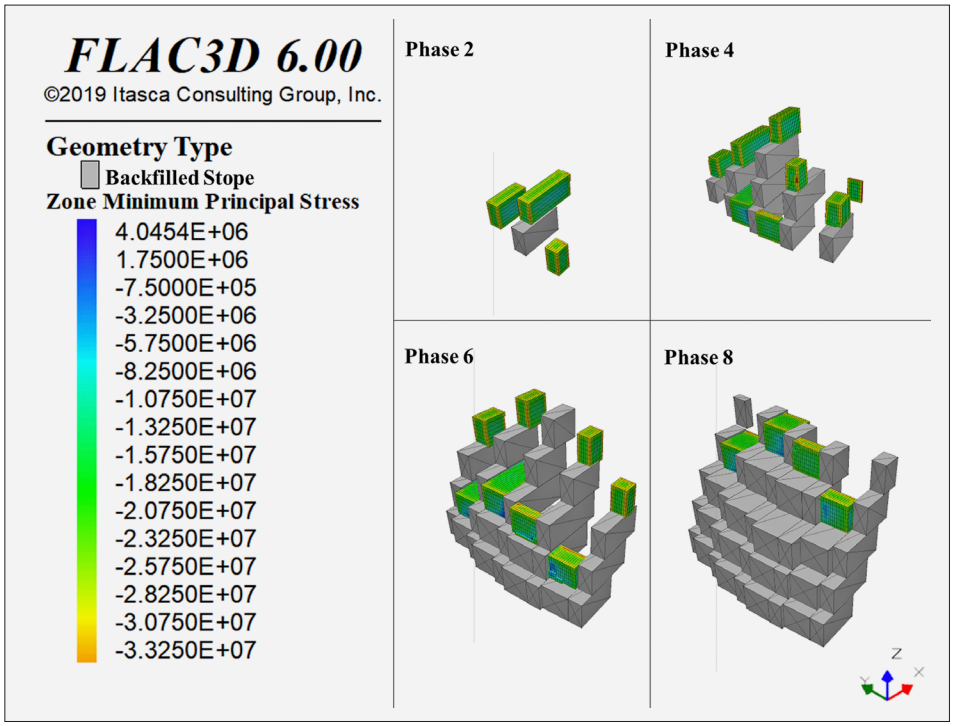

Figure 9. Stress model result

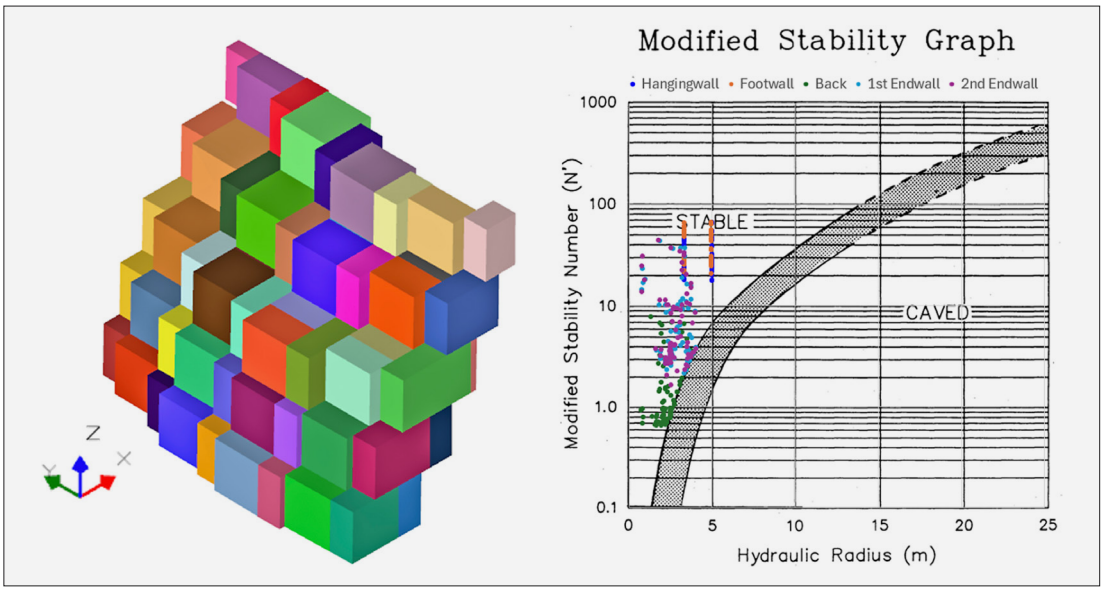

Figure 10. Final stope geometry (left) and Stability analysis (Right)

after the primary stopes in the three levels above have been mined and backfilled. The stope sequence used in this case study is illustrated in **Figure 8**. The sequence is divided into nine phases, with each phase required to be mined in the specified order.

4.3. Stress Model Result

To capture the stress changes during the stope extraction and backfilling process, stress modelling was performed using FLAC3D. The analysis was based on the representative properties of the rock mass and backfill materials. The material properties applied in the stress modelling are summarized in **Table 6**.

The modelling was performed in eight phases, following the stope mining and backfilling sequence. The maximum and minimum principal stress on each stope wall was then queried. These stress values were subsequently used to represent the stress component in the N' stability number analysis. An example of stress results from several phases is shown in **Figure 9**.

4.4. Stope Final Result

The analysis shows that the optimized stope design produced a total of 83 individual stopes, consisting of 51 secondary stopes and 32 primary stopes, shown in **Figure 10**. The stability analysis results show that all walls of each stope were in a stable condition. Several stope walls also reached their critical hydraulic radius.

The computation of the stope final results required approximately 32 minutes for the algorithm to complete the entire process, corresponding to an average of 3.1 seconds per stope slice. This computation time is deemed feasible for implementation in larger and more complex mining scenarios. The analysis was conducted on a personal computer equipped with an AMD Ryzen 9 270 (8-core) processor, an NVIDIA GeForce RTX 5080 GPU, and 16 GB of GDDR7 memory. Notably, the algorithm's running time may vary depending on the mine's complexity, the number of generated stope slices, and the device specifications.

5. Discussion

5.1. Stope Dimension Sensitivity Analysis

As described in **Section 4.1**, the geotechnical conditions are relatively complex, with high variability in rock mass strength. This variability leads to significant differences in stope stability, resulting in a wide range of optimal stope dimensions. To investigate the relationship between rock mass variability and stope geometry, a sensitivity analysis is presented in this section.

The sensitivity analysis was conducted using the calculated N' values for each stope wall orientation, as shown in **Figure 11**. The results indicate that N' values ranged from 0.5 to 90, reflecting the wide variability in potential stope dimensions. **Figure 11** further presents the percentage of samples that resulted in unstable stopes at different stope lengths. The analysis shows that stope lengths should be limited to less than 8 m to ensure that 90% of stopes remain stable. Applying a uniform stope length across all stopes would lead to higher costs and reduced production efficiency. These findings highlight the necessity of further optimization that accounts for the spatial distribution of rock mass strength, allowing stope lengths to vary according to local geotechnical conditions.

5.2. Stope Geometry Analysis

Based on the **Figure 12**, the majority of the secondary stopes have reached their maximum dimension at the

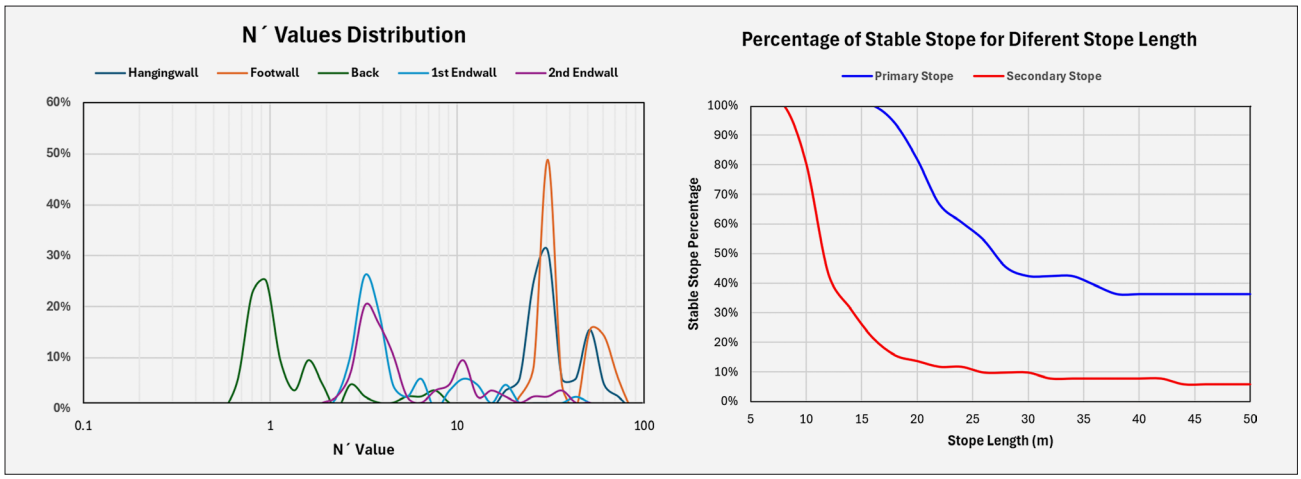

Figure 11. N' Values Distribution (left) and Percentage of Stabel Stope (right)

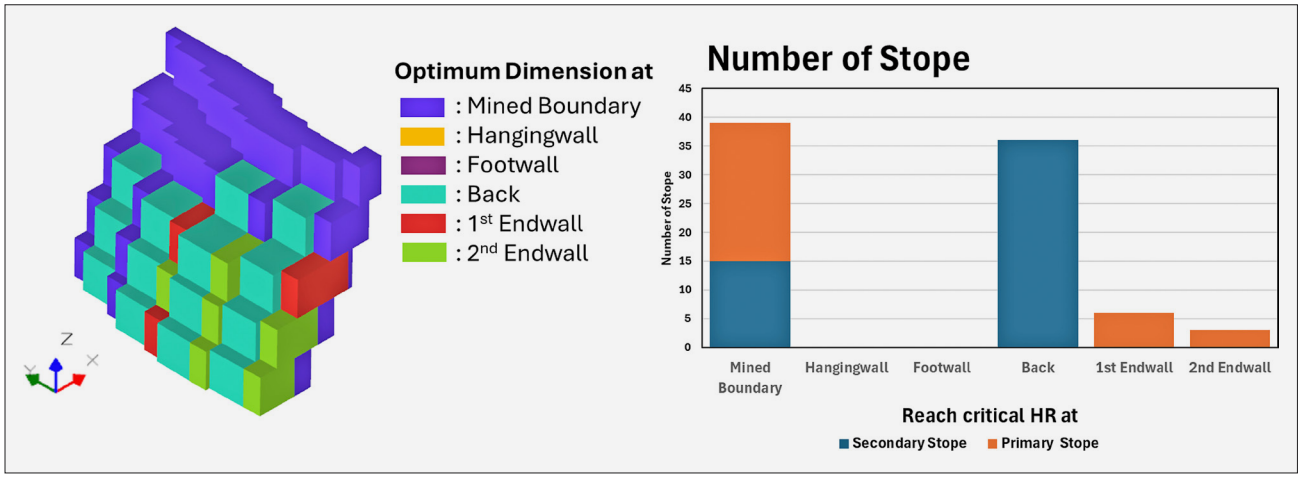

Figure 12. Critical wall of stope

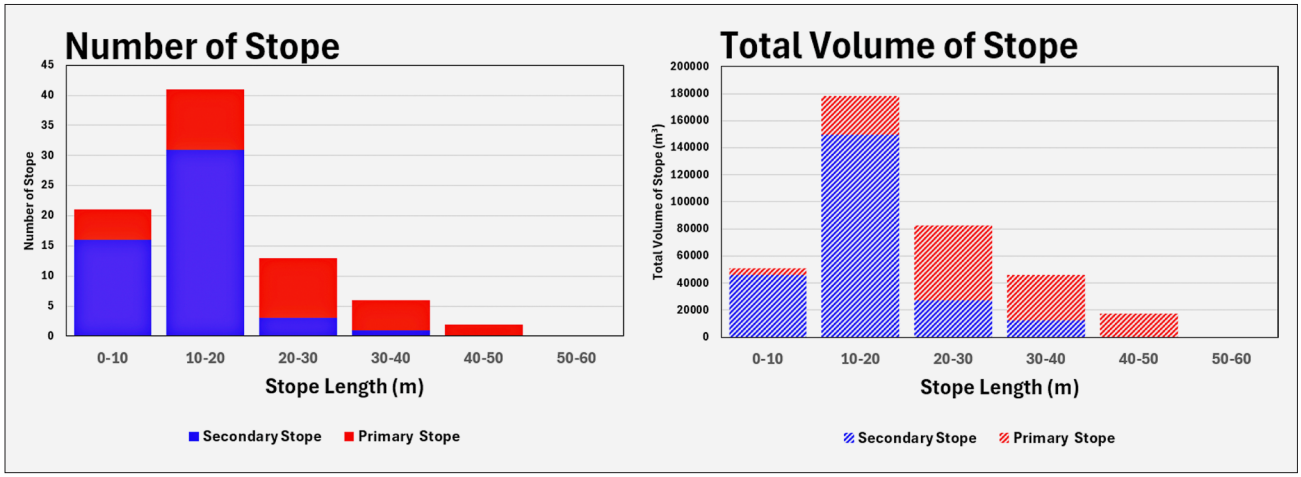

Figure 13. Distribution of Stope length

back. Meanwhile, for the primary stopes, most have reached their maximum dimension due to the mined boundary. The results also show that no stope has reached its maximum dimension at the hanging wall or footwall.

Figure 13 shows that several stopes (13% of the total volume) have a total length of less than 10 meters. Based on this result, further analysis can be conducted to evaluate the economic feasibility of these short stopes. Min-

ing small stopes can be uneconomical due to increased mining costs (**Samanta et al., 2024**).

5.3. Result Comparison

To further evaluate the effectiveness of the proposed optimization approach, a series of simulations were conducted in comparison with conventional stope design methods. These simulations incorporated varying stope length scenarios as dictated by standard design practices. The outcomes of this comparative analysis are summarized in **Table 7**, which details the performance metrics of both the conventional and optimization-based methodologies.

Table 7. Stope stability result

Method	Number of Stope	Unstable Stope
Stope produced by optimization	83	0 (0%)
Stope with regular 10m length	123	17 (14%)
Stope with regular 20m length	62	25 (40%)
Stope with regular 20m length of Primary Stope and 10m length of Secondary Stope	90	18 (20%)

The results show that the new method produces a more stable stope geometry while requiring fewer stopes. In contrast, the conventional methods, which applies a uniform stope length, results in either a more number of stopes or the presence of unstable stopes. The distribution of the unstable stopes is shown in **Figure 14**. **Figure 15** shows that most unstable face walls in regular stope scenarios occur at the back and endwall. In contrast, stopes designed using the optimization method have more adaptable HR based on the N' value, enhancing stope stability.

Stope instability frequently leads to overbreak of stope walls (**Villaescusa, 2014**), resulting in higher mining costs due to increased ore dilution. Consequently, unstable stopes are typically associated with greater dilution percentages. The empirical relationship between the hydraulic radius (HR), the modified stability number (N'), and the anticipated stope dilution is presented in **Equation 23** (**Roux, 2017**).

$$Stope\ dilution = \begin{cases} 0.6305\ln(HR) - 0.9575, & N' < 4 \\ 0.5090\ln(HR) - 0.8596, & 4 \le N' < 11 \\ 0.4144\ln(HR) - 0.4673, & 11 \le N' < 21 \\ 0.6357\ln(HR) - 1.1934, & N' \ge 21 \end{cases} \quad (23)$$

Although longer stopes are generally more susceptible to instability and increased dilution, their use can significantly reduce overall stoping costs and streamline the mining sequence. By employing longer stopes, the total number of individual stopes is minimized, which in turn lowers the requirements for slot raises and filling barricade constructions. This approach not only optimizes operational efficiency but also leads to more cost-effective production. The cost parameters utilized to compare the conventional and optimization methods are presented in **Table 8**, providing a comprehensive assessment of total stope production costs for each approach.

Table 8. Stope cost parameters

Parameters	Value	Unit
Mining cost	35.8	$/Ton
Stope slot raise and filling barricade cost (Stope Fix Cost)	43,314	$/Stope

Empirical dilution, as presented in **Equation 23** and supported by the cost parameters in **Table 8**, was utilized to calculate the expected total stope production cost for both conventional and optimization methods. **Table 9** offers a direct comparison of ore tonnage, dilution tonnage, and total stope production costs between these approaches. The results indicate that smaller stopes with a regular length of 10 meters more effectively control dilution compared to other stope dimensions, albeit at the

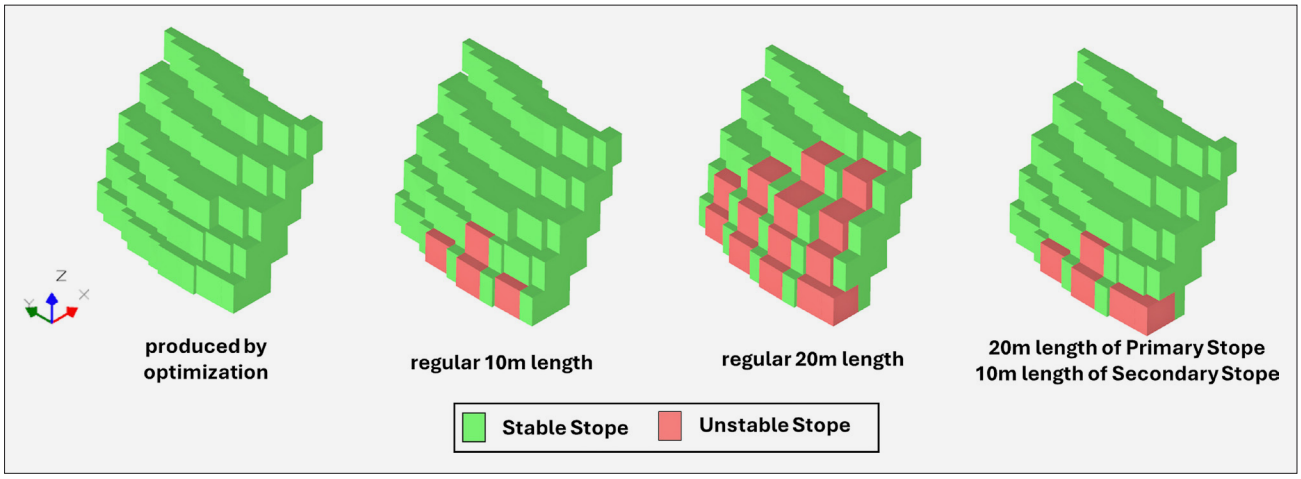

Figure 14. Distribution of Unstable Stopes

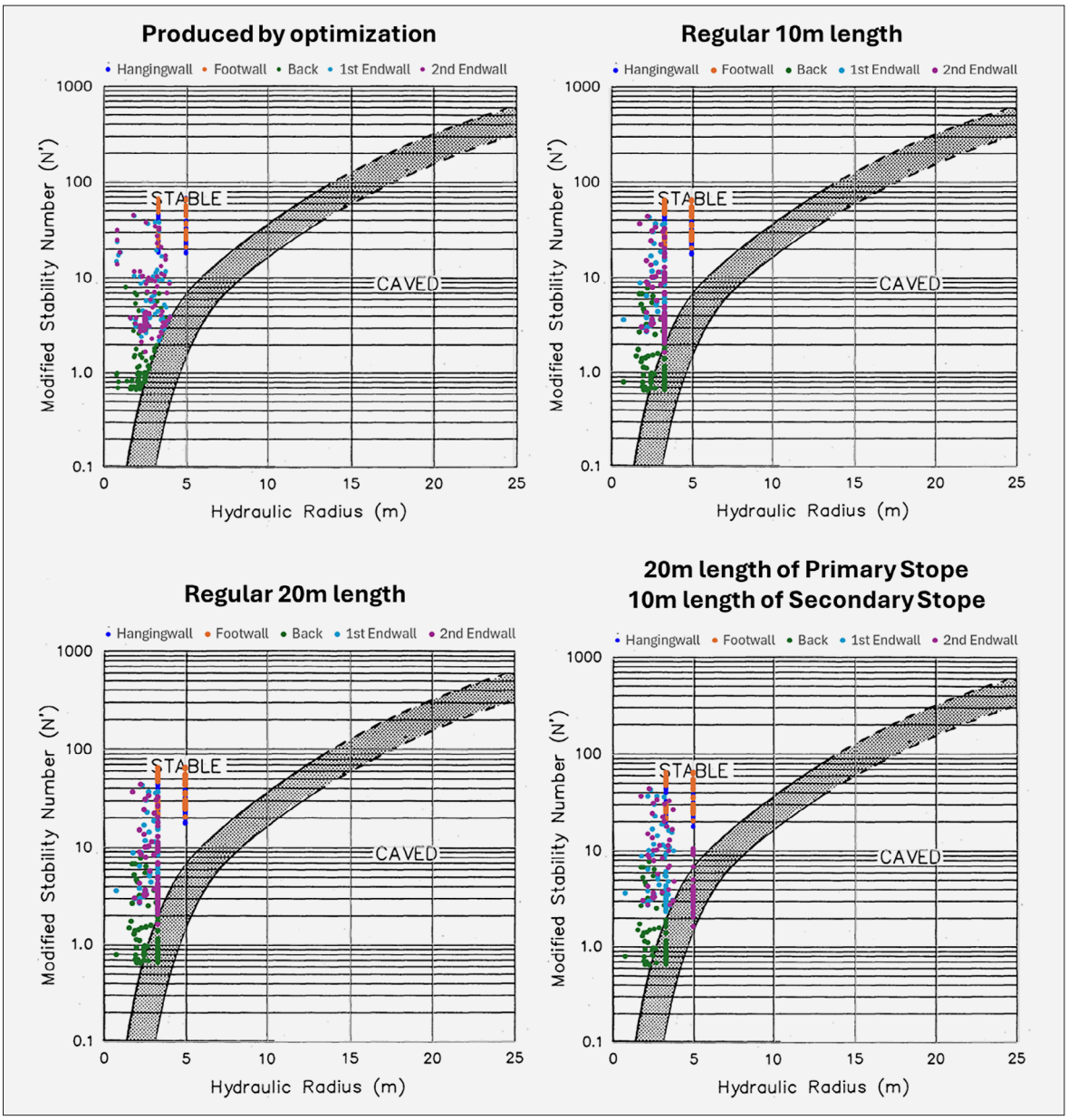

Figure 15. Stope stability analysis

Table 9. Stope dilution and production cost result

Method	Ore Tonnage	Dilution Tonnage	Average Dilution	Total Tonnage	Number of Stope	Total Stope Production Cost ($)
Stope produced by optimization	956,046	35,554	3.7%	991,600	83	39,094,326
Stope with regular 10m length	956,046	30,510	3.2%	986,556	123	40,646,328
Stope with regular 20m length	956,046	116,413	12.2%	1,072,459	62	41,079,495
Stope with regular 20m length of Primary Stope and 10m length of Secondary Stope	956,046	94,911	9.9%	1,050,956	90	41,522,490

expense of an increased number of separate stopes. Conversely, stopes configured with a 20-meter regular length exhibit the highest percentage of expected dilution, yet result in the smallest number of stopes overall. Notably, stopes produced through the optimization method demonstrate a balanced outcome in terms of dilution percentage and number of stopes. The optimized stope shapes yield the lowest total production cost, with a reduction of approximately 1.6 to 2.4 million dollars relative to the conventional method. This finding supports

the conclusion that the optimization method produces more cost-efficient stope configurations.

Stope production cost calculations, as reflected in **Table 9**, primarily account for production aspects; however, they often overlook the broader implications arising from unstable stopes. In practice, stope collapse can lead to increased expenses due to necessary rehabilitation, loss of ore reserves, and potential delays in production. Furthermore, the safety risks associated with such collapses are considerable, as they may result in equipment damage or, in extreme cases, serious injury and even fatalities. These consequences underscore the critical importance of ensuring stope stability, a goal that can be effectively achieved through optimization method. Indeed, the application of optimized stope design not only mitigates geotechnical and safety risks but may also deliver greater economic benefits than those indicated solely by the value presented in **Table 9**.

6. Conclusions

The new method shown in this research provides a more cost-efficient and adaptable approach to stope stability analysis compared to conventional method. By using an iteration on the stope dimension and conducting detailed stability assessments on each stope wall, this method allows for a more accurate evaluation of geotechnical conditions and the determination of optimized stope dimensions. Comparative analysis reveals that the proposed approach effectively reduces the total number of stopes while maintaining geotechnical stability. In contrast, traditional methods employing uniform stope lengths are prone to producing a significant proportion of unstable stopes; specifically, findings indicate that between 14% and 40% of stopes generated by conventional techniques exhibit instability. Conversely, the optimization method consistently yields stopes that satisfy stability criteria.

Furthermore, the comparative analysis underscores the ability of the optimization method to achieve an effective balance between dilution control and operational efficiency. While smaller, uniformly dimensioned stopes (e.g. 10 m length) exhibit superior dilution performance, they substantially increase the total number of stopes, thereby elevating overall production costs. In contrast, larger uniform stopes (e.g. 20 m length) minimize the number of the stopes but incur the highest dilution percentages, resulting in significant cost escalation due to increased handling of waste material. The optimized stope configurations generated by the proposed method deliver a more favourable outcome by achieving the lowest total production cost, with estimated savings of approximately USD 1.6–2.4 million compared to conventional approaches. These findings confirm that the optimization method not only enhances geotechnical stability but also provides a demonstrable economic advantage.

While the demonstrated optimization method exhibits clear advantages over conventional approaches, it is important to note that the optimization in this study was restricted to stope length. Future research can consider a comprehensive three-dimensional optimization framework that incorporates stope width and stope height, as such an approach may offer enhanced utility and further improvements in stope stability and cost efficiency.

Acknowledgement

The authors sincerely acknowledge DESWIK for granting access to their mining software, which was essential for carrying out this research.

Funding

This research was funded by Institut Teknologi Bandung through the Program Penelitian, Pengabdian Masyarakat dan Inovasi ITB.

Competing Interests

The authors have no conflicts of interest to disclose.

7. References

Adoko, A. C. (2025). Discussion on “Refined Approaches for Open Stope Stability Analysis in Mining Environments: Hybrid SVM Model with Multi optimization Strategies and GP Technique” Rock Mech Rock Eng (2024). *Rock Mechanics and Rock Engineering*. https://doi.org/10.1007/s00603-024-04348-w

Amedjoe, C. G., & Agyeman, J. (2015). Assessment of effective factors in performance of an open stope using cavity monitoring system data: A case study. *Journal of Geology and Mining Research*, *7*(3), 19–30. https://doi.org/10.5897/JGMR2014.0216

Army, M., & Karian, T. (2024). Stope Dimension Analysis Based on Geomechanical Properties Using Brute Force Algorithm. *IOP Conference Series: Earth and Environmental Science*, *1437*(1), 12032. https://doi.org/10.1088/1755-1315/1437/1/012032

Cakrabuana, W., Sadisun, I. A., Tohari, A., Dinata, I. A., Martireni, A. P., Mahmud, H. Z., & Atmojo, H. T. (2024). Andesite Slope Stability Analysis Using Rock Mass Rating (RMR) and Slope Mass Rating (SMR) in Gunung Batu and Graha Puspa Areas, West Bandung Regency, West Java, Indonesia. *Rudarsko-Geološko-Naftni Zbornik*, *39*(4), 137–151. https://doi.org/10.17794/rgn.2024.4.11

Cepuritis, P. M., Villaescusa, E., & Lachenicht, R. (2007). Back analysis and performance of Block A long hole open stopes – Kanowna Belle Gold Mine. In E. Eberhardt, D. Stead, & T. Morrison (Eds.), *Rock Mechanics: Meeting Society’s Challenges and Demands* (pp. 1431–1439). Taylor & Francis.

Chen, Q., Gan, Q., Wang, H., & Liu, C. (2024). A New Combined Mining Method: The Stope Limit Length Calculation of Considering Bulk Support Boundary. *Rock Me-*

chanics and Rock Engineering, *57*(9), 6909–6925. https://doi.org/10.1007/s00603-024-03865-y

Clark, L. M. (1998). *Minimizing dilution in open stope mining with a focus on stope design and narrow vein longhole blasting*. https://open.library.ubc.ca/collections/831/items/1.0081111

Cui, X., Yang, S., Zhang, N., & Zhang, J. (2024). Optimization of stope structure parameters by combining Mathews stability chart method with numerical analysis in Halazi iron mine. *Heliyon*, *10*(4). https://doi.org/10.1016/j.heliyon.2024.e26045

Salomon, D. (2006). Linear Interpolation. In D. Salomon (Ed.), *Curves and Surfaces for Computer Graphics* (pp. 49–69). Springer New York. https://doi.org/10.1007/0-387-28452-4_2

Diederichs, M. S., & Kaiser, P. K. (1996). Rock instability and risk analyses in open stope mine design. *Canadian Geotechnical Journal*, *33*(3), 431–439. https://doi.org/10.1139/t96-064

Dolatshahi, A., & Molladavoodi, H. (2024). Prediction of Rock Tensile Fracture Toughness: Hybrid ANN-WOA Model Approach. *Rudarsko-Geološko-Naftni Zbornik*, *39*(3), 1–12. https://doi.org/10.17794/rgn.2024.3.1

Guo, Y., & Miao, Y. (2022). Study on stope stability in continuous mining of long-dip, thin orebody by room–pillar method. *Sustainability*, *14*(15), 9601.

Heidarzadeh, S., Saeidi, A., & Rouleau, A. (2019). Evaluation of the effect of geometrical parameters on stope probability of failure in the open stoping method using numerical modeling. *International Journal of Mining Science and Technology*, *29*(3), 399–408. https://doi.org/10.1016/j.ijmst.2018.05.011

Heidarzadeh, S., Saeidi, A., & Rouleau, A. (2020). Use of probabilistic numerical modeling to evaluate the effect of geomechanical parameter variability on the probability of open-stope failure: a case Study of the Niobec Mine, Quebec (Canada). *Rock Mechanics and Rock Engineering*, *53*(3), 1411–1431.

Kang, Q., Wang, Y., Zhang, S., Pu, C., & Zhang, C. (2021). Prediction of Stope Stability Using Variable Weight and Unascertained Measurement Technique. *Geofluids*, *2021*(1), 8821168. https://doi.org/10.1155/2021/8821168

Li, C., Liu, G., Guo, L., Zheng, D., & Yuan, X. (2024). A New CRITIC-GRA Model for Stope Dimension Optimization Considering Open Stoping Stability, Mining Capacity and Costs. *Applied Sciences*, *14*(12). https://doi.org/10.3390/app14125249

Mathews, K. E., Hoek, E., Wyllie, D. C., & Stewart, S. B. V. (1980). Prediction of stable excavations for mining at depths below 1000 metres in hard rock. *Canmet Report*, *802*, 1571.

McFadyen, B., Grenon, M., Woodward, K., & Potvin, Y. (2024). Optimising stope design through economic and geotechnic assessments of predictions made at a meter scale resolution using the sites' reconciled data. *International Journal of Rock Mechanics and Mining Sciences*, *178*, 105778. https://doi.org/10.1016/j.ijrmms.2024.105778

Nhleko, A. S., & Musingwini, C. (2022). Optimisation of Three-Dimensional Stope Layouts Using a Dual Interchange Algorithm for Improved Value Creation. *Minerals*, *12*(5). https://doi.org/10.3390/min12050501

O'Hara, T. A., & Suboleski, S. C. (1992). Chapter 6:3: Costs and Cost Estimation. In H. L. Hartman (Ed.), *SME Mining Engineering Handbook* (2nd ed., Vol. 1, pp. 405–424). Society for Mining, Metallurgy, and Exploration (SME).

Patanwar, Y. K., Mohanto, S., & Deb, D. (2025). Stability Analysis of Deep Underground Stopes with Transverse Method of Extraction Using 3-Dimensional Numerical Modelling Technique. In A. K. Gorai, S. Ram, R. M. Bishwal, & S. Bhowmik (Eds.), *Sustainable and Innovative Mining Practices* (pp. 427–441). Springer Nature Switzerland.

Phaisopha, S., Shimada, H., Sasaoka, T., Hamanaka, A., Pongpanya, P., Shorin, S., & Senthavisouk, K. (2023). A Stope Mining Design with Consideration of Hanging Wall When Transitioning from Open Pit Mining to Underground Mining for Sepon Gold Mine Deposit, Laos. *Mining*, *3*(3), 463–482. https://doi.org/10.3390/mining3030027

Potvin, Y. (1988). *Empirical open stope design in Canada* [University of British Columbia]. https://doi.org/10.14288/1.0081130

Press, W. H., Teukolsky, S. A., Vetterling, W. T., & Flannery, B. P. (2007). *Numerical Recipes: The Art of Scientific Computing* (3rd ed.). Cambridge University Press.

Putra, D., Karian, T., Sulistianto, B., & Heriawan, M. N. (2024). Integrating Mathews Stability Chart into the Stope Layout Determination Algorithm. *Mining, Metallurgy & Exploration*, *41*(3), 1351–1364. https://doi.org/10.1007/s42461-024-00993-5

Rinne, M., Janiszewski, M., Pontow, S., Uotinen, L., Kiuru, R., Kangas, L., Laine, I., & Leveinen, J. (2024). Improvements in Rock Mass Description for Stope Design by Geophysical and Geochemical Methods. *Applied Sciences*, *14*(3). https://doi.org/10.3390/app14030957

Roux, P. J. (2017). Value creation in a mine operating with open stoping mining methods. *Journal of the Southern African Institute of Mining and Metallurgy*, *117*, 133–142. https://doi.org/10.17159/2411-9717/2017/v117n2a4

Sabao, A. R., Munemo, P., & Kolapo, P. (2022). Investigating the causes of stope instability at Golden Valley Mine. *Journal of Sustainable Mining*, *21*(2), 128–140.

Samanta, G., Sinha, S., & Dey, T. (2024). A Case Study on Economic Impact Assessment of Developing Single Drill Level in Sublevel Stoping Method. *Journal of The Institution of Engineers (India): Series D*, *105*(1), 119–125. https://doi.org/10.1007/s40033-023-00453-2

SME. (2011). *SME Mining Engineering Handbook, Third Edition* (D. Peter, Ed.). Society for Mining, Metallurgy, and Exploration.

Stephenson, R. M., & Sandy, M. P. (2013). Optimising stope design and ground support – a case study. In Y. Potvin & B. Brady (Eds.), *Ground Support 2013: Proceedings of the Seventh International Symposium on Ground Support in Mining and Underground Construction* (pp. 387–400). Australian Centre for Geomechanics.

Sugianti, K., & Tohari, A. (2023). The Impact of Geological and Rainfall Characteristics on Slope Stability Analysis in

Shallow Landslide Modelling using the TRIGRS Model. *Rudarsko-Geološko-Naftni Zbornik*, *38*(4), 147–166. https://doi.org/10.17794/rgn.2023.4.12

Villaescusa, E. (2014). *Geotechnical Design for Sublevel Open Stoping*. https://doi.org/10.1201/b16702

Zadhesh, J., & Majdi, A. (2022). Estimation of Rock Joint Trace Length Using Support Vector Machine (SVM). *Rudarsko-Geološko-Naftni Zbornik*, *37*(3), 55–64. https://doi.org/10.17794/rgn.2022.3.5

Zhang, Q., Huang, M., & Guo, J. (2024a). A Simulation Analysis of the Stability of Tall and Collapse-Prone Stopes: A Case Study of the Dongguashan Copper Mine. *Applied Sciences*, *14*(22). https://doi.org/10.3390/app142210608

Zhao, X., & Zhou, X. (2023). Design Method and Application of Stope Structure Parameters in Deep Metal Mines Based on an Improved Stability Graph. *Minerals*, *13*(1). https://doi.org/10.3390/min13010002

Zhou, X., Zhao, X., Qu, Q., & Shi, J. (2023). Stope Structural Parameters Design towards Green and Deep Mining: A Review. *Processes*, *11*(11). https://doi.org/10.3390/pr11113125

Zulfahmi, Z., Sarah, D., Novico, F., & Susilo, R. B. (2023). Assessment of Rock Slope Stability in a Humid Tropical Region: Case Study of a Coal Mine in South Kalimantan, Indonesia. *Rudarsko-Geološko-Naftni Zbornik*, *38*(2), 109–125. https://doi.org/10.17794/rgn.2023.2.8

SAŽETAK

Optimizacija dimenzija komora u geotehnički složenome rudniku primjenom automatizirane analize stabilnosti

Stabilnost komora i stupova jedan je od ključnih čimbenika u podzemnoj eksploataciji mineralnih sirovina pomoću komorno-stupne metode jer izravno utječe na sigurnost, produktivnost i ukupnu ekonomsku učinkovitost proizvodnje. Tradicionalne metode projektiranja komora često se temelje na uniformnim dimenzijama, pri čemu se zanemaruje geotehnička varijabilnost ležišta, što povećava rizik od pojave nestabilnosti ili neoptimalnih dimenzija komora i stupova. U ovome radu predlaže se pristup automatizirane analize stabilnosti koji iterativno procjenjuje različite varijante dimenzioniranja komora na temelju modificiranoga koeficijenta stabilnosti (N') s ciljem određivanja optimalne stabilne konfiguracije. Provođenjem detaljnih analiza stabilnosti za svaki zid komore i međustup, metoda omogućuje znatno precizniju procjenu stvarnih geotehničkih uvjeta u usporedbi s konvencionalnim metodama uniformnih dimenzija. Studija slučaja pokazala je da predloženi pristup omogućuje smanjenje ukupnoga broja komora uz održavanje potrebne razine stabilnosti za razliku od klasičnih metoda kod kojih 14 – 40 % komora pokazuje znakove nestabilnosti. Nadalje, optimizacija omogućuje postizanje povoljnoga kompromisa između kontrole razrjeđenja i operativne učinkovitosti, što rezultira nižim troškovima eksploatacije po komori. Optimizirane konfiguracije ostvarile su najniži ukupni trošak proizvodnje uz procijenjene uštede od približno 1,6 – 2,4 milijuna USD u odnosu na konvencionalne projekte. Dobiveni rezultati potvrđuju da okvir optimizacije ne samo da poboljšava geotehničku stabilnost komorno-stupnoga sustava, već donosi i znatne ekonomske prednosti naglašavajući važnost uvažavanja geotehničke varijabilnosti u projektiranju komora i stupova.

Ključne riječi:
stabilnost komora, komorno-stupna metoda, modificirani faktor stabilnosti N', optimizacija dimenzija komora, automatizirana analiza

Author's contribution

Mohammad Army (MS Scholar): Conceptualization, writing – review and editing, software, visualization, and project administration. **Tri Karian** (PhD, Lecturer): validation, methodology, formal analysis, writing – review and editing. **Firly Rachmaditya Baskoro** (PhD, Lecturer)**, Takashi Sasaoka** (PhD, Lecturer) and **Akihiro Hamanaka** (PhD, Lecturer): resources, writing – review and editing, validation, supervision, and funding acquisition. **Budi Sulistianto** (PhD, Lecturer) and **Hideki Shimada** (PhD, Lecturer): validation, resources, supervision, writing – review and editing.
All authors have read and agreed to the published version of the manuscript.